Integrative Transcriptomic, and Proteomic Analysis of Flavonoid Biosynthesis During Fruit Maturation In Chinese Raspberry "*Rubus Chingii* Hu"

Xiaobai Li (hufanfan1982815@gmail.com)
Institute of Horticulture https://orcid.org/0000-0001-9615-3543
Jian Sun
Zhejiang Research Institute of Traditional Chinese Medicine Co.,Ltd
Jingyong Jiang
Taizhou Academy of Agricultural Sciences
Zhen Chen
Taizhou University
Aaron Jackson
Aaron Jackson South Oak, Stuttgart AR 72160

Research Article

Keywords: Antioxidants, Anthocyanin, Flavonoid, Gene, Enzyme, Chinese raspberry

Posted Date: March 13th, 2021

DOI: https://doi.org/10.21203/rs.3.rs-284541/v1

Abstract

Rubus chingii, is a red-fruited species of *Rubus* native to China, which is a popular and nutritious fruit in China. However, change in flavonoid composition and content during fruit maturation is poorly understood. This study examined flavonoids and the genes/proteins during four fruit ripening phases using LC-MS/MS. As a result, six major kinds of anthocyanins were first identified in *R. chingii*, which primarily consisted of flavanol-anthocyanins, are new to *Rubus*. Apart from anthocyanins, concentrations of fruit flavonoids were much higher than most berries including raspberries, and it is this that contributes to their high phenolic concentrations and antioxidant capabilities. In contrast to other known raspberries, *R. chingii* had a decline in flavonoids during fruit maturation, which was due to down-regulation of genes/proteins involved in phenylpropanoid and flavonoid biosynthesis. Surprisingly, anthocyanin continuously decreased during fruit coloration. This suggests that anthocyanins are not responsible for the fruit's reddish coloration. The biosynthesis of these flavanol-anthocyanins consumed two flavonoid units both produced through the same upstream pathway. Their presence indicates a reduction in the potential biosynthesis of anthocyanin production. Also, the constantly low expression of RcANS gene down-regulated overall anthocyanin biosynthesis. The lack of RcF3'5'H gene/protein hindered the production of delphinidin glycosides. Flavonoids primarily comprising of quercetin/kaempferol-glycosides were predominately located at fruit epidermal-hair and placentae. The profile and biosynthesis of *R. chingii* flavonoids are unique to *Rubus*. It could be used to broaden the genetic base of raspberry cultivars and to improve their fruit quality.

Introduction

Rubus chingii Hu (Chinese raspberry), Chinese name "Fu-Pen-Zi", is indigenous to China, and mainly distributed along the lower-middle reaches of the Yangtze River. Like red raspberry (*R. idaeus* L., subgenus *Idaeobatus* Focke), blackberry (*Rubus* sp., subgenus *Rubus* L.), and black raspberry (subgenus *Idaeobatus*), it is highly appreciated by consumers not only for its special flavor but also for its nutritional properties due to the abundant antioxidants.

Plant flavonoids mainly consist of anthocyanins, condensed and hydrolyzable tannins. These flavonoids contribute to the taste, flavor, and color of food and drink, e.g. astringency and/or color, and have a wide of pharmaceutical uses, such as its astringent action. Prior studies have extensively examined *Rubus* flavonoids. For example, anthocyanin compositions have been identified and quantified in raspberries. Red and black raspberry share the same profile of anthocyanins. Their anthocyanins are predominantly cyanidin glycosides (e.g. glucosides, sophorosides, rutinosides, sambubioside and glucosyl-rutinosides), but they only contain low to trace levels of pelargonidin glycosides (Kula et al. 2016; Ludwig et al. 2015; Mazur et al. 2014). Black raspberry has up to five-fold greater anthocyanin content than red raspberry (Krauze-Baranowska et al. 2014). Flavonols in red and black raspberry are mainly kaempferol/quercetin glycosides with glucosides, rutinoside and coumaroylglucoside (Kula et al. 2016). Moreover, agricultural technologies, elicitors, stimulating agents and plant activators, have been applied to increase *Rubus* flavonoid content (Jin et al. 2012). In *R. chingii*, previous phytochemical studies have isolated a series of flavonoids (Ding 2011; Guo et al. 2005). The flavonoids dramatically change as the fruit ripens, which has attracted considerable research attention. However, to our knowledge, few studies have been conducted on flavonoid change and their biosynthesis during maturation in *R. chingii*. This study was undertaken to investigate the change in composition and content of flavonoids, and explore potential mechanisms underlying flavonoid biosynthesis during fruit maturation based on the genetic and enzymatic components.

Materials And Methods

Plant Material.

R. chingii Hu fruits were collected from five to six plants at varying maturation phases i.e. mature green (MG), green yellow (GY), Yellow orange (YO) and Red (RE) during the growing season (May, 2019) at LINHAI, Zhejiang, China (Fig. 1a). Fruits were collected and immediately frozen in liquid nitrogen then stored in a -70°C freezer. Ten fruits were pooled as one replicate. Three biological replicates were used for all experiments. The fruit were ground in liquid nitrogen into powder and subsequently used for analysis of mRNA, protein and metabolites. The content measurements of composition were determined relative to overall fruit weight.

Total anthocyanin, carotenoid flavonoid, phenolic content and ABTS assays.

Total anthocyanin content was determined via spectrophotometry. Fruit tissue was ground in liquid nitrogen. Approximately 0.3 g of tissue were weighed and added to 10 mL 1% (*v*/*v*) HCl methanol (HCl and methanol: Shanghai Hushi Chemical, Shanghai, China) and incubated for 24 h at room temperature in the dark. After centrifugation for 15 min at 13,000 × g, supernatants were measured for absorbance at 530, 620 and 650 nm. The anthocyanin content was estimated using the following formulas:

$$\Delta A = (A530 - A620) - 0.1 \times (A650 - A620)$$

The anthocyanin content = $\Delta A \times V \times M / (\varepsilon \times m)$

Where V is the extract volume (mL), ε is the molar extinction coefficient of cyanidin-3-glucoside at 530 nm (29600), M is the molecular weight of cyanidin-3-glucoside (449 g mol^{-1}), and m is the mass of the fruit extracted. The results were expressed as cyanidin-3-glucoside equivalents (mg/g FW).

Total content of carotenoid was determined via spectrophotometry. Sample fruit were grounded in liquid nitrogen and approximately 0.3 g tissue (ground powder) was mixed with 10 ml extraction solution (ethanol:acetone = 1:2). The extraction was vortexed and then put in darkness for at least half hr until the residues became colorless. The absorbance of the extractive solvent was measured at 440, 645 and 663nm for carotenoid, and chlorophyll a/b respectively.

Chlorophyll a (mg/g FW) = 0.01× (12.7× A663−2.69 × A645) × V/(M×1000);

Chlorophyll b (mg/g FW) = 0.01× (22.9× A645–4.68 × A663) × V/(M×1000);

Total Chlorophyll (mg/g FW) = (20.21× A645 + 8.02 × A663) × V/(M×1000);

Carotenoids (mg/g FW) = 4.695 A 440–0.268 [Chlorophyll (a + b)] × V/(M×1000)];

Total flavonoid content was quantified by a colorimetric assay method. Fruit tissue was completely ground with liquid nitrogen. Approximately 0.3 g of tissue was weighed, mixed with 10 mL ethanol for 2 h at room temperature in the dark, and centrifuged for 15 min at 3000 rpm. One mL of supernatant was mixed with 2.4 mL ethanol and 0.4 mL $NaNO_2$ (Sangon Biotech, Shanghai, China). After incubation for 6 min, the mixture was added to 0.4 mL 10% $Al(NO_3)_3$ solution (Sangon Biotech, Shanghai, China). After an additional 6 min, the mixture was added to 4 mL 4% NaOH and brought to volume of 10 mL with 100% ethanol. After 15 min at room temperature the absorbance was determined at 510 nm and measured relative to a blank extraction solvent. A calibration curve was prepared using rutin solution (8–48 μg/mL). Total flavonoid content was expressed as rutin (China national analytical center, Guangzhou, China) equivalent (mg/g FW).

Total phenolic content was determined using the Folin-Ciocalteu method following the procedure (Li et al. 2019). Fruit tissue was completely ground with liquid nitrogen. Approximately 0.3g of tissue was weighed, mixed with 10 mL of acidified methanol (0.1% hydrochloric acid) for 24 h in the dark and centrifuged for 15 min at 3000 rpm. The extract was appropriately diluted to fall in the range of the standard curve, 2 mL of which was transferred to another colorimetric tube, mixed with 1 mL 0.5 N Folin-Ciocalteu's phenol reagent (Sigma-Aldrich, Shanghai, China), and allowed to react for 5 min at room temperature. The reaction was neutralized with 2 mL of 5% saturated Na_2CO_3 and incubated for 60 min at 30 ℃. The absorbance was measured at 760 nm. A calibration curve was prepared using gallic acid solution (5-100 μg/mL). TPCs were expressed as gallic acid (Sigma-Aldrich, Shanghai, China) equivalent (mg/g FW).

The free radical-scavenging activity was determined using the ABTS radical cation decolorization method (Jin et al. 2016). Fruit tissue was ground in liquid nitrogen. Approximately 0.3g of tissue was weighed and added to H_2O. ABTS radical cation (ABTS+) was obtained by mixing 7.0 mmol/L ABTS solution (Roche, Shanghai, China) with 2.45 mmol/L potassium persulfate at 2:1 (v/v) and stored in the dark at room temperature for at least 16 h. The ABTS•+ solution was diluted with 80% ethanol until its absorbance reached 0.700 ± 0.02 at 734 nm. The ABTS•+solution (4.0 mL, absorbance of 0.700 ± 0.02) was thoroughly mixed with 0.1 mL appropriately diluted fruit aqueous extract. The mixture was placed at room temperature for 6 min, and its absorbance was immediately measured at 734 nm. A standard curve was obtained using a gradient of Trolox (Sigma-Aldrich, Shanghai, China) concentrations (50–900 mol/L). Results were expressed at TEAC (mmol/g FW).

Frozen sections and Flavonoid In situ DPBA staining

The fresh fruits were chopped into several parts and embedded in SCEM embedding medium (Section-Lab, Hiroshima, Japan). The targeted tissue was embedded until the surface was tightly covered with adhesive film and then immediately frozen at − 20°C. The frozen samples in embedding medium were trimmed and then carefully sliced to produce 50–80 μm fresh-frozen sections using a CM1850 Cryostat (Leica microsystems, Wetzlar, Germany) set at − 20°C.

The sections of fruit were stained in a freshly prepared aqueous solution of 0.25% (w/v) 2-aminoethyl diphenylborate (DPBA) (Tokyo Chemical industry, Tokyo, Japan) and 0.00375% (v/v) Triton X-100 (Sigma-Aldrich, Shanghai, China) for at least 30 min. A Zeiss LSM880 confocal laser scanning microscope (Carl Zeiss AG, Jena, Germany) was used to excite the roots with 30% maximum laser power at 458 nm, and the fluorescence was collected at 475–504 nm for kaempferol and 577 to 619 nm for quercetin (Lewis et al. 2011).

Total RNA extraction, library construction, and bioinformatic analysis

Fruit RNAs were extracted by CTAB method, their quality was tested with an Agilent 2100 Bioanalyzer (Agilent RNA 6000 Nano Kit) (Agilent, Santa Clara, CA, USA) for RNA concentration, RIN value, 28S/18S ribosomal RNA and the fragment length distribution. The RNA purity was determined using a NanoDrop™ (Thermo Fisher Scientific, Wilmington, USA).

The libraries construction followed the method described in Li et al. (Li et al. 2013). The mRNAs were isolated from total RNA with oligo(dT) and then fragmented. The first and second strand of cDNA were synthesized, purified and resolved with EB buffer for end repair and adenine (A) addition. After that, the cDNA fragments were connected with adapters and those with suitable size were PCR amplified. Agilent 2100 BioanayIzer and ABI StepOnePlus Real-Time PCR System (Thermo Fisher Scientific, Rockford, USA) were used to quantify and qualify the libraries.

The read data were processed following the procedure (Li et al. 2013). The low-quality reads (> 20% of the bases with low quality < 10) and reads with adaptors and unknown bases (N > 5%) were filtered to get clean reads. The clean reads were assembled into unigenes using Trinity, for functional annotation and expression estimation. Data are available via NCBI with accession (PRJNA671545). The relative expression was estimated by Fragments Per Kilobase of transcript per Million mapped reads (FPKM). Based on the relative expression, differential expressed unigenes were defined by threshold (fold Change > 2.00 or < 0.5; adjusted P value < 0.05) and they were subjected to pathway enrichment (FDR < 0.01 are defined as significant enrichment).

Protein extraction, HPLC fractionation, LC-MS/MS assay and bioinformatic analysis

Fruit proteins were extracted by the method described by Li et al. (Li et al. 2019; Li et al. 2020). The concentration was determined using a BCA protein assay kit (Thermo Fisher Scientific, Rockford USA). The extracted proteins were reduced, and then digested by trypsin. After trypsin digestion, peptides were desalted and processed as TMT10plex™ Isobaric Label Reagent (Thermo Fisher Scientific, Rockford, USA).

The labeled peptides were fractionated by HPLC, and the peptides were divided into 18 fractions. The peptides were loaded into tandem mass spectrometry (MS/MS), Orbitrap Fusion™ Tribrid™ (Thermo Fisher Scientific, Rockford, USA). These processes were performed as described by Li et al. (Li et al. 2019; Li et al. 2020). The relative expression of isoform was estimated by comparing the intensities of the reporter ions. Compared to the expression profile at the MG phase, differential expressed isoforms were defined by threshold change (change fold > 1.5 or < 0.67 and P < 0.05).

The resulting shotgun MS/MS data were processed using a Maxquant search engine (v.1.5.2.8), and searched against the transcriptomic data concatenated with a reverse decoy database (Li et al. 2019). Data are available via ProteomeXchange with identifier (PXD021977). KEGG enrichment of isoforms were determined by a two-tailed Fisher's exact test. The significant threshold was set up (p-value < 0.05) for KEGG enrichment.

Analysis of major anthocyanins and flavonoids

Anthocyanins were extracted with 1% (v/v) HCl methanol and concentrated by CentriVap refrigerated Centrifugal Concentrators at 8℃ (Models 73100 Series) (Labconco, Kansas City, USA) and then re-dissolved it with 1 mL 1% (v/v) HCl methanol. Flavonoids was extracted with 70% methanol for 2 h at room temperature in the dark, and refrigerated Centrifugal Concentrators at 8℃ (Labconco Models 73100 Series) and then re-dissolved it with 1 mL 70% methanol. The extract was passed through a 0.22-μm microporous membrane filter for LC-MS analysis.

For anthocyanins, the mobile phases were 1% formic acid-water (A) and acetonitrile (B). Gradient conditions were as follows: 0–25 min, 5–35% phase B; 25-37min; 35–95% phase B. The loading volume was 5 μL, the flow rate was 0.4 mL min^{-1}; the column temperature was 50℃, and the UV detector was set at 530 nm. For flavonoids, the mobile phases were 0.1% formic acid-water (A) and 0.1% formic acid-acetonitrile (B). The linear gradient programs were as follows, 0–5 min, 5–10% phase B; 5-25min, 10–25% phase B; 25-37min, 25–95% phase B; Sample injection volume was 5μL; Column oven temperature was 50℃; Flow rate was 0.3mL min − 1; and the UV detector was set at 360 nm. Anthocyanins and flavonoids separated by UPLC was analyzed using a MS AB Triple TOF 5600^{plus} System (AB SCIEX, Framingham, USA) in both negative ion (source voltage at -4.5 kV, and source temperature at 550 ℃) and positive ion mode (source voltage at + 5.5 kV, and source temperature at 600 ℃). Maximum allowed error was set to ± 5 ppm. Declustering potential (DP), 100 V; collision energy (CE), 10 V. For MS/MS acquisition mode, the parameters were almost the same except that the collision energy (CE) was set at 40 ± 20 V, ion release delay (IRD) at 67 and the ion release width (IRW) at 25. The IDA-based auto-MS^2 was performed on the 8 most intense metabolite ions in a cycle of full scan (1 s). The scan range of m/z of precursor ion and product ion were set as 100-2,000 Da and 50 − 2,000 Da. The exact mass calibration was performed automatically before each analysis employing the Automated Calibration Delivery System.

Results

Changes of anthocyanins, flavonoids, phenolics and antioxidant capability

Total anthocyanin was relatively low, ranging from 6.92 (mg /100 g FW) in RE to 19.52 in MG. As fruit matured, anthocyanin surprisingly decreased by 19.37%, 36.56%, and 30.72% from MG to GY, to YO, and to RE (Fig. 1c). Based on dry weight, anthocyanin content also showed a trend of decrease (Table 1). Total content of flavonoids ranged from 128.50 (mg RE/100 g FW) in RE to 646.20 in MG, and it decreased by 42.05%, 55.26%, and 23.31% from MG to GY, YO, and RE (Fig. 1e). Similarly, total content of phenolics ranged from 760.83 (mg GAE/100 g FW) in RE to 4,026.25 in MG. Phenolic content dropped by 39.01%, 54.68%, and 31.64% from MG to GY, YO, and RE respectively (Fig. 1d). In contrast, total carotenoids increased by 5.84%, 11.96% and 43.58% from the MG to GY, YO, and RE phases (Fig. 1b).

Table 1
Change of water content and anthocyanin concentration (DW) during fruit ripening

Phase	Fresh weight (g)	±	SD	Dry weight (g)	±	SD	Water content	Anthocyanin (mg/100 g DW)
MG	1.06	±	0.06	0.39	±	0.02	63.67%	53.72
GY	1.39	±	0.08	0.45	±	0.02	67.63%	48.62
YO	1.91	±	0.1	0.46	±	0.03	75.92%	41.46
RE	4.78	±	0.15	0.9	±	0.06	81.11%	36.62
MG: mature green; GY: green yellow; YO, yellow orange; RE: red.								
Anthocyanin concentration (DW): Anthocyanin concentration (FW) was multiplied by fresh weight, and then divided by dry weight.								
DW: dry weight; FW: fresh weight								

Total antioxidant capacity of fruit was estimated by the free radical-scavenging activity (ABTS) assay. ABTS ranged from 10.05 (mmol TEAC/100 g FW) in RE to 41.18 in MG and it dropped by 33.74%, 45.78% and 32.06% from MG to GY, YO, and RE (Fig. 1f). There were high Pearson correlation coefficients between these parameters ranging from 0.968 to 0.999, and averaging 0.986 (Fig. 1g). The results indicate the flavonoids are one of the most important phenolic compositions that contribute to total antioxidant capacity.

Fruit flavonoids composition, anatomical structure and flavonoid staining during fruit maturation

In *R. chingii*, anthocyanin primarily consisted of monomeric, and dimeric anthocyanins (Fig. 2a, b and c; Fig. S3). Of these anthocyanins, four had flavanol-anthocyanin condensed forms (dimeric anthocyanins) and pelargonidins were the main type of anthocyanin aglycones. All of condensed forms contained a flavan-3-ol [either (epi)afzelechin or (epi)catechin] as the upper unit carbon–carbon linked to a lower anthocyanin unit consisting of different anthocyanin derivatives (Fig. S3). (Epi)afzelechins were the common monomeric precursors (flavan-3-ols) of the flavanol-anthocyanin. The glycosides of

(epi)afzelechin(4α->8)pelargonidin were the most abundant type (Fig. 2d, e and f). These anthocyanins all significantly decreased in content during fruit ripening, which was consistent to the change in content of total anthocyanin. Also, major flavonoids consisted primarily of glycosides of quercetin and kaempferol. Of these flavonoids, kaempferol-3-o-rutinoside was predominant, followed by ellagic acid and kaempferol-3-glucoside. All them significantly decreased in content during fruit ripening, which was in accordance with the change in content of total flavonoids.

A raspberry fruit is an aggregate fruit composed of drupelets (Fig. 3a). Each drupelet contains the pericarp and seed. The pericarp is made up of the exocarp, hypodermis, and mesocarp layers; while the seed consists of the episperm, endosperm, and embryo. The exocarp is attached with a layer of epidermal hair and the seed is surrounded by placentae. In fruit cross-sections, DPBA fluorescence showed flavonoid accumulation patterns at various stages of fruit maturation (Fig. 3b). Each flavonoid-DPBA conjugate was labeled by a unique fluorescent color (kaempferol by yellow and quercetin by red). Flavonol-specific fluorescence was mainly observed in the fruit epidermal hair throughout the entire fruit maturation process, but rarely in fruit flesh including the exocarp, hypodermis and mesocarp (Fig. 3c, d, e, and f). As fruit matured, fruit epidermal hair became shorter and thinner. In addition, flavonol-specific fluorescence was seen in the placentae and seed coats of developing seed (Fig. 3c, d, d, and f). The results suggest that the majority of flavonoids are concentrated in fruit epidermal hair and placentae.

Profiling of genes and proteins involved in flavonoid synthesis

Twelve transcriptomics were developed for BG, GY, YO and RE fruits. A total of 89,188 unigenes were obtained, and 49,755 (55.79%) and 37,833 (42.42%) were annotated in non-redundant and KEGG database respectively. The biggest difference in gene expression was between RE/MG (6,502 up-regulated and 5733 down-regulated unigenes) while the smallest difference was between GY/MG (1,965 up-regulated and 1,966 down-regulated unigenes) (Fig. S1a). Accordingly, in twelve proteomes of BG, GY, YO and RE fruits, 141,036 unique peptides corresponding to 9,478 isoforms, and 8,529 quantified isoforms were identified. In proteomics, the most difference in isoform expression (506 up-regulated and 618 down-regulated isoforms) was observed between RE/MG while the smallest difference was between GY/MG (765 up-regulated and 799 down-regulated isoforms) (Fig. S1b). In metabolomics, 8,218 high quality ions included 7,611 (92.61%) ions with relative standard deviation (RSD) < = 30% in positive ion mode, while 6,150 high quality ions included 4,683 (76.15%) ions with RSD < = 30% in negative ion mode. The largest difference detected (1,656 and 1024 in positive and negative ion modes respectively) was between RE/MG while the smallest difference was between GY/MG (2,151 and 1,468 in positive and negative ion modes respectively) (Fig. S1c). The results suggest that a large number of genes, proteins, and metabolites are involved in fruit maturation, and the biggest difference is between RE and MG while the smallest difference is between GY and MG.

Generally, flavonoid products are involved in four pathways, i.e. “phenylpropanoid biosynthesis”, “flavonoid biosynthesis”, “flavone and flavonol biosynthesis”, and “anthocyanin biosynthesis”. KEGG enrichment was performed to discern the multivariate pattern of up- and down-regulated unigenes/isoforms. The unigenes involved in “phenylpropanoid biosynthesis” and “flavonoid biosynthesis” were significantly enriched in GY/MG, YO/MG and RE/MG and most of them were down-regulated (Fig. S2a). Accordingly, the down-regulated isoforms involved in these pathways’ biosynthesis were enriched as well (Fig. S2b). However, neither up-regulated or down-regulated unigenes/isoforms were enriched in “flavone and flavonol”, or “anthocyanin” biosynthesis (Fig. S2). This suggests that “phenylpropanoid biosynthesis” and “flavonoid biosynthesis” are more active in green phases than the other three phases, and responsible for biosynthesis of major flavonoid products during fruit maturation.

Differentially expressed gene and protein in flavonoid and phenylpropanoid biosynthesis

In transcriptomics, 608 unigenes were predicted to be involved in phenylpropanoid biosynthesis, flavonoid biosynthesis, flavone and flavonol biosynthesis, and anthocyanin biosynthesis, and 309 (50.82%) were differentially expressed. A large part of unigenes were maintained at low expression level during fruit maturation. In our proteomics study we identified 116 isoforms involved in these pathways and 55 (47.41%) were differentially expressed. These isoforms were all mapped to their corresponding unigenes, but a large number of isoforms corresponding to these unigenes could not be detected. The inconsistencies between unigenes and isoforms may be due to the discrepancy of transcriptomic and proteomic techniques such as differences in detectable threshold.

In phenylpropanoid biosynthesis the main enzymes included pheammonia lyase (PAL), cinnamate-4-hydroxylase (C4H), 4-coumaroyl-CoA synthase (4CL) and chalcone synthase (CHS). Two PAL homologs, RcPAL (Unigene4740 and Unigene4485), were phylogenetically grouped together (Fig. S4a) and significantly down-regulated at the gene/protein level during maturation (Table 2; Fig. 4a and b). Rc4CL and Rc4CL-like homologs were phylogenetically grouped into two branches respectively (Fig. S4b). The 4CL homologs were significantly down-regulated at the gene/protein level during maturation. Rc4CL-like homologs (CL7730.Contig2, CL3087.Contig1, and 8828.Contig1) had low gene expression and their proteins were not detected (Table 2; Fig. 4a and b). Two C4H homologs, RcC4H (Unigene9842, and Unigene12468), were phylogenetically grouped into two different branches i.e.C4H1 and C4H2, respectively (Fig. S4c), but they had a trend of down-regulation at the gene/protein level during maturation (Table 2; Fig. 4a and b). CHS homologs were grouped together (Fig. S4d) and down-regulated at the gene/protein level during maturation (Table 2; Fig. 4a and b). These up-stream genes/proteins were down-regulated to decrease conversion from phenylpropanoids to flavonoids.

Table 2
The temporal change in expression of mRNA unigenes and Protein isoforms involved in phenylpropanoid, flavonoid and anthocyanin bio

	mRNA unigenes														Protein isoforms		
	MG			GY				YO				RE				MG		G
	Mean	±	SD	Mean	±	SD		Mean	±	SD		Mean	±	SD		Mean	±	SD
RcPAL(Unigene4740)	1448	±	38.35	372.9	±	21.61	*	82.76	±	2.74	*	43.93	±	1.25	*	1.79	±	0.04
RcPAL(Unigene4485)	261.8	±	2.12	52.63	±	6.36	*	9.16	±	1.74	*	3.25	±	0.2	*	2.05	±	0.13
Rc4CL(CL2617.Contig1)	193.5	±	4.78	49.16	±	3.54	*	31.24	±	1.51	*	30.05	±	1.34	*	1.85	±	0.04
Rc4CL(CL6300.Contig1)	264	±	4.91	138.9	±	2.67	*	74.06	±	1.42	*	81.89	±	1.34	*			
Rc4CL(CL6300.Contig2)	235.5	±	11.2	143.7	±	10.47	*	70.4	±	2.52	*	67.14	±	3.21	*	1.41	±	0.03
Rc4CL(CL8627.Contig1)	263.4	±	4.6	143.2	±	2.01	*	20.65	±	1.35	*	1.75	±	0.43	*	1.71	±	0.04
Rc4CL-like(CL7730.Contig2)	3.65	±	0.48	1.14	±	0.24	*	0.42	±	0.12	*	0.04	±	0.04	*			
Rc4CL-like(CL3087.Contig1)	1.82	±	0.08	6.02	±	0.32	*	5.49	±	0.49	*	0.86	±	0.24	*			
Rc4CL-like(8828.Contig1)	3.28	±	0.19	3.85	±	0.62		4	±	0.17		6.62	±	0.85				
RcC4H(Unigene9842)	692.5	±	12.81	284.2	±	10.64	*	124.2	±	3.25	*	338.8	±	6.83	*	1.64	±	0.02
RcC4H(Unigene12468)	274.9	±	25.84	109.3	±	6.21	*	38	±	0.76	*	7.18	±	0.53	*	1.51	±	0.01
RcCHS(CL6140.Contig1)	740.4	±	56.75	43.19	±	7.71	*	21.58	±	1.69	*	13.36	±	0.73	*			
RcCHS(CL6140.Contig2)	234.5	±	36.02	18.67	±	7.56	*	4.24	±	0.22	*	1.69	±	1.24	*			
RcCHS(CL6140.Contig4)	238.6	±	26.79	25.21	±	3.14	*	4.08	±	0.82	*	1.61	±	0.7	*			
RcCHS(CL6140.Contig5)	938.4	±	87.82	68.39	±	19.58	*	21.93	±	1.95	*	12.82	±	0.19	*	2.01	±	0.06
RcCHI(Unigene14858)	293	±	3.94	69.41	±	3.83	*	37.66	±	0.29	*	48.17	±	1.53	*	1.82	±	0.02
RcCHI(Unigene22344)	100.8	±	1.58	22.08	±	0.32	*	6.96	±	0.66	*	2.18	±	0.31	*	2.66	±	0.04
RcDFR(Unigene24396)	116.2	±	6.36	15.79	±	5.04	*	8.31	±	0.48	*	4.45	±	0.06	*			
RcDFR(CL2475.Contig1)	56.67	±	2.72	9.29	±	1.79	*	4.39	±	0.7	*	1.26	±	0.03	*			
RcDFR(CL2475.Contig4)	41.22	±	2.74	4.93	±	0.88	*	3.12	±	0.05	*	0.99	±	0.13	*			
RcDFR(CL2475.Contig5)	50.94	±	0.36	3.44	±	0.22	*	0.59	±	0.13	*	0.36	±	0.11	*			
RcDFR(CL2475.Contig7)	53.15	±	1.39	2.54	±	0.18	*	0.52	±	0.08	*	0.11	±	0.05	*			
RcF3H(CL7001.Contig2)	367.1	±	2.13	136	±	14.02	*	48.14	±	3.59	*	9.98	±	0.74	*	1.92	±	0.05
RcF3'H(Unigene19522)	10.76	±	0.7	1.67	±	0.63	*	0.15	±	0	*	2.53	±	0.28	*			
RcFLS(Unigene22291)	8.17	±	1.6	1.98	±	0.69	*	0.57	±	0.29	*	1.07	±	0.23	*			
RcFLS-like(Unigene52413)	2.96	±	0.16	5.17	±	0.66		5.44	±	3.03		3.37	±	0.18				
RcFLS-like(Unigene52414)	4.99	±	0.78	5.03	±	0.17		8.87	±	2.34		6.96	±	0.54				
RcFLS-like(CL3345.Contig2)	3.56	±	0.56	3.95	±	0.05		5.89	±	0.35		4.63	±	0.72				
RcANR2(Unigene7245)	27.39	±	3.01	6.86	±	2.01	*	3.39	±	0.05	*	2.67	±	0.65	*	1.81	±	0.08
RcANR3(Unigene17647)	0.1	±	0.1	1.47	±	0.06	*	1.68	±	0.02	*	0.06	±	0.06				
RcANR3(Unigene27757)	0	±	0	0	±	0		0.43	±	0.43		0	±	0				
RcLAR(CL9527.Contig2)	0.36	±	0.36	1.01	±	0.58		0.12	±	0.12		0	±	0				
RcLAR(CL9527.Contig3)	93.98	±	10.29	3.06	±	1.18	*	1.53	±	0.17	*	0.41	±	0.06	*	2.28	±	0.34
RcANS/LODX(Unigene7480)	0.79	±	0.2	3.41	±	0.21	*	0	±	0		5.82	±	0.49	*			
RcBZ1/UGT78D-1(Unigene7678)	43.82	±	4.66	4.17	±	0.65	*	0.12	±	0.06	*	0.03	±	0.03	*	1.87	±	0.12
RcBZ1/UGT78D-1(Unigene22174)	32.5	±	2.41	4.21	±	0	*	0.84	±	0.09	*	0.11	±	0	*	1.95	±	0.05
RcBZ1/UGT78D-2(Unigene7056)	2.79	±	0.01	3.52	±	0.05		3.9	±	0.36		0.3	±	0.03		1.10	±	0.02

	mRNA unigenes														Protein isoforms			
	MG			GY				YO				RE				MG			G
	Mean	±	SD	Mean	±	SD		Mean	±	SD		Mean	±	SD		Mean	±	SD	
RcBZ1/UGT78D-2(CL3164.Contig1)	8.11	±	0.48	12.61	±	0.73		22.92	±	1.19	*	16.59	±	0.19	*	0.81	±	0.09	
Rc3GGT /UGT79B(CL2207.Contig1)	0.18	±	0	0.55	±	0.32		0.09	±	0.09		0.05	±	0.05					
Rc3GGT /UGT79B(CL2207.Contig2)	2.92	±	0.47	4.83	±	1.47		1.4	±	0.06		0.01	±	0.01					
Rc3GGT /UGT79B(CL2207.Contig3)	6.2	±	0.38	6.46	±	0.47		5.06	±	0.13		0.42	±	0.24		1.09	±	0.08	
Rc3GGT /UGT79B(CL2207.Contig4)	0.72	±	0.01	1.41	±	0.04		0.57	±	0.02		0.13	±	0.08					
Rc3GGT /UGT79B(CL2207.Contig5)	0.8	±	0.15	0.35	±	0.14		0.79	±	0.14		0.88	±	0.05					
Rc3GGT /UGT79B(Unigene4033)	0.97	±	0.21	1.11	±	0.23		0.25	±	0.09		0.49	±	0.16					
Rc3GGT /UGT79B(Unigene4034)	1.68	±	0.04	2.71	±	0.59		1.17	±	0.01		0.23	±	0.08					
RcGT1(CL10466.Contig1)	7.05	±	0.11	6.82	±	0.59		4.53	±	1.22		0.6	±	0.45					
RcGT1(CL10466.Contig3)	9.96	±	0.72	7.4	±	0.54		6.96	±	0.42		9.9	±	1.47					
RcGT1(CL1924.Contig1)	21.29	±	0.12	68.02	±	5.49	*	86.88	±	2.18	*	53.47	±	2.1	*	0.77	±	0.03	
RcGT1(CL1924.Contig3)	2.08	±	0.05	1.4	±	0.23		0.58	±	0.06		1.59	±	0.09					
RcGT1(Unigene268)	1.89	±	0.05	1.07	±	0.25		1.15	±	0.25		0.82	±	0.09					
*: significant difference with fold Change > 2.00 or < 0.5 and adjusted P value < 0.05 for unigenes; with fold > 1.5 or < 0.67 and P < 0.05 for protein isoform																			
Different homologs were designed with different serial numbers, e.g. two homologs, RcPAL(Unigene4740) and RcPAL(Unigene4485)																			

In flavonoid biosynthesis, the main enzymes included chalcone isomerase (CHI), flavanone-3-hydroxylase (F3H), flavonoid-3'-hydroxylase (F3’H), flavonoid-3’,5’-hydroxylase (F3’5’H), flavonol synthase (FLS), bifunctional dihydroflavonol 4-Reductase/flavanone 4-Reductase (DFR), flavonoid glycosyltransferases (UFGT). CHI homologs were phylogenetically separated into two different branches i.e. CHI1 and CHI2 respectively (Fig. S4e) and both of them were down-regulated at gene/protein level during maturation (Table 2; Fig. 4a and b). Five DFR unigenes, belonging to one DFR homolog, were phylogenetically grouped into the DFR branch (Fig. S4f) and significantly down-regulated during maturation (their proteins were not detected) (Table 2). F3H and F3’H homologs each with one unigene were phylogenetically grouped into the F3H and F3’H branch respectively, but neither RcF3’5’H unigene nor isoform was detected (Table 2, Fig. S4g). RcF3H (CL7001.Contig2) were significantly down-regulated at the gene/protein level during maturation, while the RcF3'H (Unigene19522) unigene was maintained at a low level and its isoform was not detected. FLS homologs were respectively separated into FLS and FLS-like groups (Fig. S4h). The FLS-like group was represented by FLS paralogs without a conserved functional domain (Fig. S4l). FLS-like homologs were all maintained at low gene expression and none of their isoforms were detected. However, RcFLS (Unigene22291) showed a decreasing trend of gene expression but remained expressed at low levels (Table 2, Fig. 4a). These genes/proteins were down-regulated, reducing the biosynthesis of flavone, flavonol and their derivates. Notably, a deficiency of RcF3’5’H blocked the conversion from dihydroquercetin to dihydromyricetin, resulting in the absence of leucodelphinidin, myricetin, (epi)gallocatechin and delphinidin glycoside.

In anthocyanin biosynthesis, the main enzymes included anthocyanidin reductase (ANR), leucoanthocyanidin reductase (LAR), leucoanthocyanidin dioxygenase (ANS/LODX) and anthocyanidin 3-*O* glucoside 5-*O* glucosyltransferase (GT1). The RcANS/LODX homolog was maintained at low gene expression and its protein was not detected (Table 2). RcLAR (CL9527.Contig3) and RcANR2 (Unigene7245) were both significantly down-regulated at the gene/protein level during maturation. (Table 2; Fig. 4a and b; Fig. S4i and j). In contrast, RcANR3 (Unigene17647 and Unigene27757), had very low gene expression and their corresponding proteins were not detected. Three main class of glucosyltransferase were identified i.e. anthocyanidin 3-*O*-glucosyltransferase (BZ1/UGT78D), anthocyanidin 3-*O*-glucoside 2"-*O*-glucosyltransferase (3GGT/UGT79) and anthocyanidin 5,3-*O* glucosyltransferase (GT1). A phylogenetic tree grouped these glucosyltransferase homologs into three main branches (Fig. S4k). Two homologs, BZ1/UGT78D-1 and BZ1/UGT78D-2, had different patterns of expression (Table 2; Fig. 4). RcBZ1/UGT78D-1 (Unigene7678 and Unigene22174) were significantly down-regulated at the gene/protein level as fruit matured, while RcBZ1/UGT78D-2 (Unigene7056) remained constantly expressed at both the gene/protein level and the RcBZ1/UGT78D-2 (CL3164.Contig1) gene/protein was slightly up-regulated. There were three homologs for each Rc3GGT/UGT79 and RcGT1, but they had relatively low expression and did not show a clear trend of change at the gene/protein level. The consistently low level of expression of RcANS suggests a relatively low concentration of anthocyanins. Notably, the genes/proteins of RcLAR and RcANR2 were highly expressed in unripe fruit, resulting in the relative abundance of flavan-3-ols, i.e. (epi)catechinand and (epi)afzelechin. These flavan-3-ols were interacted with each other or with cyanin/pelargonin to generate proanthocyanins or dimeric anthocyanins respectively.

In conclusion, most of the differently expressed unigenes/isoforms in these pathways shared a similar trend of change in expression, which was consistent with the high correlations seen between them (Pearson correlation = 0.956). However, the phylogenetically different homologs shows different patterns of gene/protein expression. The results suggest the changes observed in gene expression are consistent with those seen in protein expression and the homologs are divergent in function.

Discussion

Changes in flavonoids and their localization during fruit maturation

It was surprising to see that the total anthocyanin, flavonoids, and phenolics all showed a continuous decrease during the fruit maturation process in *R. chingii*. This pattern was different from any previous report in *Rubus* species including red/black raspberry. In red raspberry, anthocyanin concentration continuously increases throughout fruit ripening, but the total phenolic concentration decreases from the green to the veraison stage, and then increases until maturity (Wang et al. 2009). Cyanidin-3-*O*-sophoroside is the most prominent anthocyanin followed by cyanidin-3-*O*-rutinoside and cyanidin-3-*O*-glucoside (Stavang et al. 2015). The flavonols, hyperoside and quercetin-3-*O*- glucoside are both constantly present at low concentrations (Stavang et al. 2015). In black raspberry, the content of flavonols e.g. quercetin 3-*O*-rutinoside and quercetin-glucuronide, and anthocyanins e.g. cyanidin 3-*O*-xylosylrutinoside and cyanidin 3-*O*-rutinoside increases during ripening, while the content of flavanols, (epi)catechin and B type proanthocyanidin dimers decrease (Hyun et al. 2014). The increasing trend of anthocyanins and the “V”-type change of total phenolics are ubiquitous during maturation in many berries, e.g. blueberry (Li et al. 2019), cranberries (VvedenskayaVorsa 2004), strawberry (Song et al. 2015), and grape (Giribaldi et al. 2007), which is mainly due to their substantial increase in anthocyanin pigment concentration after veraison (Li et al. 2019). In *R. chingii*, the continuous down-regulation of total flavonoids (including anthocyanins) was responsible for the continuous decrease of phenolics. These pigments primarily consisting of an anthocyanin linked to a flavonol, were first reported in *Rubus* species. Interestingly, fruit anthocyanins decreased inversely with its red coloration during maturation, which indicates that its red coloration is caused by something other than anthocyanins. For example, the accumulation of carotenoids as the fruit maturates may be responsible for the red coloration (Fig. 1B).

R. chingii fruit is very high in antioxidants, which is highly correlated with the phenolic compounds including flavonoids. In *R. chingii*, total content of phenolics peaked at 4,026.25 (mg GAE/100 g FW) in MG (Fig. 1b). It is 10 fold higher than mature fruit in red raspberry (357.83 mg GAE/100 g FW), blackberry (850.52), strawberry (621.92), blueberry (305.38) and cherry (314.45) (Chen et al. 2013; De Souza et al. 2014). Even at the lowest concentration in the RE stage, total phenolic content was 760.83 (mg GAE/100g FW), which was much higher than most of the other fruits (Chen et al. 2013; De Souza et al. 2014). Also, total content of flavonoids peaked at 646.20 in MG (mg RE/100g FW), which was higher than that in raspberry (Chen et al. 2013)(Fig. 1d). Similarly, ABTS peaked at 41.18 (mmol TEAC/100g FW) or 411.80 (umol TEAC/g FW) in MG and was over 20 fold higher than mature fruit of red raspberry (6.27 umol TEAC/g FW), blackberry (13.23), strawberry (7.87), blueberry (5.88) and cherry (8.83) (De Souza et al. 2014). The lowest content of ABTS in the RE stage of *R. Chingii* was 100.52 (umol TEAC/g FW), which was still 10-fold higher than the previously mentioned fruits. The extremely high antioxidant capacity could be a valuable natural source of antioxidants for use in the food industry

Flavonoid in situ staining shows that the flavonoids (i.e. kaempferol and quercetin derivates) predominately accumulate at the same tissues (epidermal hair and placentae) of fruits during the four typical maturation phases. It is highly likely that these flavonoids are synthesized in the cells in which they accumulate. The flavonoids in epidermal hair might function as antioxidants that protect fruit from pests and pathogens, while the ones in seed may function as endogenous regulators of auxin transport that is responsible for seed maturation. As the fruit maturated the epidermal hairs became thinner and shorter and many of them fell off. The epidermal hair loss could be also related to the decrease of flavonoids (Fig. 2c and d)

Down-regulated expression of genes/proteins in the phenylpropanoid pathway caused a decrease in flux from phenylpropanoids to flavonoids

The genes and enzymes involved with the phenylpropanoid biosynthesis and the flavonoid biosynthesis have been extensively studied in many plants. Most of these genes are involved in multigene families. Some members are divergent in function and others are redundant or underutilized (Kim et al. 2004). In *Arabidopsis*, two redundant PAL genes (AtPAL1 and AtPAL2) are both expressed in vascular tissues. AtPAL3 is primarily expressed in roots and leaves, albeit at low levels, while AtPAL4 is mainly expressed in developing seed tissue (Raes et al. 2003). These divergent PAL genes respond differentially under various developmental events and environmental stresses (Chang et al. 2008; Cochrane et al. 2004; KumarEllis 2001). In tomato, only one PAL transcript is induced by pathogen or wounding (Chang et al. 2008). In red raspberry, RiPAL1 is expressed during early fruit ripening, while RiPAL2 is expressed at later stages of flower and fruit development (KumarEllis 2001). PAL genes also show tissue specific patterns of expression. The expression of RiPAL1 transcripts is much higher than that of RiPAL2 in leaves, shoots, roots, young fruits, and ripe fruits. In blueberry, three PAL genes are up-regulated at the gene/protein level as fruit matures (Li et al. 2019). In this study, two phylogenetically close RcPALs were both down-regulated at the gene/protein level as fruit matured (Fig. S4a; Fig. 4a and b).

4CL isoenzymes exhibit distinct substrate affinities due to their different metabolic functions. In *Arabidopsis*, four 4CL genes are divergent in functions e.g. At4CL4 exhibits the rare property of activating sinapate and other 4CL substrates (e.g. 4-coumarate, caffeate, and ferulate) (HambergerHahlbrock 2004). In *Physcomitrella patens*, three 4CLs display the highest catalytic efficiency towards 4-coumarate, which is distinguished from the fourth 4CL (Silber et al. 2008). In blueberry, Vc4CL and Vc4CL-like are both up-regulated as fruit maturates although they are phylogenetically separated (Li et al. 2019). In this study, two phylogenetically distant CL4 homologs (RcCL4 and Rc4CL-like) showed distinct patterns of expression (Table 2). 4CLs were significantly down-regulated at the gene/protein level as fruit maturated while 4CL-like genes were expressed at low levels. The results suggest that 4CL rather than 4CL-like functions in down-regulation of the phenylpropanoid pathway in fruit.

C4H belongs to a large group of cytochrome P450 monooxygenases (P450) in plants and exclusively constitute the CYP73 family, a typical group of P450. In citrus, C4H1 and C4H2 are different in both expression patterns and N-termini, suggesting they have specific functions in organelles (Betz et al. 2001). In

blueberry, two phylogenetically close C4H homologs (VcC4H2A and VcC4H2B) are dramatically up-regulated from the pink to blue phase (Li et al. 2019). In this study, two phylogenetically related RcC4H homologs (Unigene9842 and Unigene12468) both had down-regulated expression.

Regulation of genes/proteins in flavonoid biosynthesis are responsible for the diversity in flavonoid composition and concentration

Different CHS genes are associated with the different phenotypes. In Ipomoea, six CHS genes are regulated by developmental signals. Of these, CHSD and CHSE function in flavonoid biosynthesis, especially CHSD which has dominant effects on floral pigmentation (Clegg et al. 2000). In blueberry, three phylogenetically close CHS genes share a similar pattern of up-regulation (Li et al. 2019). In Korean black raspberry, two CHS genes are both up-regulated during fruit maturation (Hyun et al. 2014). However, in *R. chingii*, the opposite occurs and one of the RcCHS is down-regulated at the gene/protein level during fruit maturation. Chalcone isomerase (CHI) is a rate-determining enzyme in flavonoid biosynthesis. In red-fruited tomato the CHI gene is expressed at low levels and decreases upon ripening while an accompanying accumulation of the CHI substrate, naringenin chalcone, occurs (Bovy et al. 2002). Heterologous expression of petunia CHI gene in tomato results in up to 70-fold increase in flavonols in the fruit peel, and a decrease in naringenin chalcone (Muir et al. 2001). In grape, CHI gene expression gradually decreases with ripening, and later, slightly increases (Wang et al. 2012). In Korean black raspberry, three CHI genes were all up-regulated during fruit maturation (Hyun et al. 2014). Here, two classes of RcCHI (Fig. S4e) were both down-regulated at the gene/protein level during fruit maturation (Fig. 4).

F3H, F3'H, F3'5'H and FLS play an important role in the types and quantities of flavonoid biosynthesis, which determines the colors and flavors of fruits (Li et al. 2019). In blueberry, F3H, F3'5'H and FLS are all up-regulated at the gene/protein level during fruit maturation (Li et al. 2019). In Korean black raspberry, two F3H genes are both up-regulated during fruit maturation (Hyun et al. 2014). In contrast, RcF3H was down-regulated at the gene/protein level during fruit maturation. Moreover, the gene expression of RcF3'H, and RcFLS were low and down-regulated during ripening. Interestingly, the absence of RcF3'5'H in *R. chingii* impeded biosynthesis of myricetin and delphinidin glycoside. The results suggest that the low expression or down-regulation of these genes/proteins reduces biosynthesis of dihydroflavonol and flavonols, while a deficiency of RcF3'5'H reduces the forms that are produced.

DFR is responsible for branch flux from dihydroflavonol into anthocyanin while ANR and LAR converts anthocyanidin leucoanthocyanidins to flavan-3-ols and then to proanthocyanidins (condensed tannins). DFR genes in Korean black raspberry (Hyun et al. 2014) and DFR proteins in blueberry (X. Li et al., 2019) are all up-regulated at the gene/protein level as the fruit matured. In contrast, two classes of RcDFR genes were significantly down-regulated during fruit maturation. In blueberry, LAR protein is up-regulated during fruit maturation (Li et al. 2019). The opposite occurred in *R. chingii* with down regulation of RcLAR at the gene/protein level during fruit maturation (Table 2, Fig. 4). The results indicate that the down-regulated expression of RcDFR is responsible for the decrease of leucoanthocyanidins while the down-regulated expression of RcLAR and RcANR is responsible for the decrease of flavanols. However, the flavanols, i.e. (epi)catechin and (epi)afzelechin could be combined with pelargonin for production of dimeric anthocyanins. Notably, the biosynthesis of dimeric anthocyanins requires two flavonoid units, rather than a single flavonoid unit as is needed with monomeric anthocyanins. One unit is produced from a shunt of anthocyanin biosynthesis while the other is from a shunt of flavanols biosynthesis, but both shunts share a common upstream pathway. In *R.chingii*. two different shunts indicate a reduction in the potential biosynthesis of these dimeric anthocyanin. Also, the constantly low expression of RcANS causes a reduction in overall anthocyanin biosynthesis.

Flavonoid glycosyltransferases have roughly four different functional classes including 3-*O*, 5-*O*, 7-*O* glycosyltransferases and diglycoside/disaccharide chain glycosyltransferases, respectively. 3-*O* glycosyltransferase includes AtUGT78D1 and AtUGT78D2 in *Arabidopsis* (Kim et al. 2012), and CsUGT78A14 and CsUGT78A15 in *Camellia sinensis*, which are responsible for biosynthesis of flavonol 3*O*glucosides/galactosides, respectively (Cui et al. 2016). 5-*O* glycosyltransferase includes AtUGT75C1 (anthocyanins 5-*O* glucosyltransferase) in *Arabidopsis* (Gachon et al. 2005), and CsUGT75L12 (flavonoid 5-O glycosyltransferases) (Dai et al. 2017). 7-*O* glycosyltransferase includes AtGT-2 (flavonoid 7*O*glucosyltransferase) in *Arabidopsis* (Kim et al. 2006), and GmIF7GT (UDP-glucose:isoflavone 7*O*glucosyltransferase) (Noguchi et al. 2007). Moreover, there is another class of flavonoid glycosyltransferases, i.e. flavonol 3-*O*-glycoside: 2"-*O* glucosyltransferase (3GGT/UGT79), an enzyme responsible for the terminal modification of pollen-specific flavonols (Knoch et al. 2018). In blueberry, two 3-*O* glycosyltransferase genes are both up-regulated as fruit matured, while another 5-*O* glycosyltransferase is down-regulated (Li et al. 2019). In Korean black raspberry four 3-*O* glycosyltransferase genes are all up-regulated as fruit matured. In *R. chingii*, two 3-*O* glycosyltransferases (RcBZ1/UGT78D) were all down-regulated at the gene/protein level as the fruit matured, while 5-*O* glycosyltransferase and flavonol 3-*O*-glycoside: 2"-*O* glucosyltransferase genes were mostly maintained at low expression levels. The results indicate that the down-regulation of 3-*O* glycosyltransferase is responsible for the decreased content of flavonol glycosides (e.g. kaempferol-3-*O*-glucoside, quercetin 3-*O*-glucoside) (Fig. 2d, e and f). A diversity in flavonoid glycosyltransferases leads to a variety of flavonoid glycosides, e.g. flavonoid coumaroylglucoside, flavonoid rutinoside, flavonoid sophoroside etc.

Conclusion

R. chingii Hu had much higher antioxidant capabilities than other berries including raspberries, which is partly due to its abundance in flavonoids (but not anthocyanins). Most of flavonoids were located at fruit epidermal-hair and placentae. In most berries there is an increase in the total flavonoid and anthocyanin concentration near the end of the fruit maturation. However, in *R. chingii* the unripe (mature green) fruit had much higher flavonoid levels, as well as anthocyanin concentrations, than was seen in latter phases of fruit development. Notably, most of anthocyanins were in flavanol-anthocyanin condensed forms, which have not been previously reported in *Rubus*. The lower flavonoid and anthocyanin concentrations in latter phases of *R. chingii* fruit development is due to the down-regulation of phenylpropanoid, and flavonoid biosynthesis. These mechanisms appear to be unique to *R. chingii*, and have not been reported in other fruit crops. Multiple genes and proteins in these pathways were divergent in function and differently regulated.

References

Betz C, McCollum TG, Mayer RT (2001) Differential expression of two cinnamate 4-hydroxylase genes in `Valencia' orange (Citrus sinensis Osbeck). Plant Mol Biol 46(6):741–748

Bovy A, de Vos R, Kemper M, Schijlen E, Almenar Pertejo M, Muir S, Collins G, Robinson S, Verhoeyen M, Hughes S, Santos-Buelga C, van Tunen A (2002) High-flavonol tomatoes resulting from the heterologous expression of the maize transcription factor genes LC and C1. Plant Cell 14(10):2509–2526

Chang A, Lim MH, Lee SW, Robb EJ, Nazar RN (2008) Tomato phenylalanine ammonia-lyase gene family, highly redundant but strongly underutilized. J Biol Chem 283(48):33591–33601

Chen L, Xin X, Zhang H, Yuan Q (2013) Phytochemical properties and antioxidant capacities of commercial raspberry varieties. Journal of Functional Foods 5(1):508–515

Clegg MT, Durbin ML, Ayala FJ, Fitch WM, Clegg MT (2000) Flower color variation: a model for the experimental study of evolution. Proc Natl Acad Sci U S A 97(13):7016

Cochrane FC, Davin LB, Lewis NG (2004) The Arabidopsis phenylalanine ammonia lyase gene family: kinetic characterization of the four PAL isoforms. Phytochemistry 65(11):1557–1564

Cui L, Yao S, Dai X, Yin Q, Liu Y, Jiang X, Wu Y, Qian Y, Pang Y, Gao L, Xia T (2016) Identification of UDP-glycosyltransferases involved in the biosynthesis of astringent taste compounds in tea (Camellia sinensis). J Exp Bot 67(8):2285–2297

Dai X, Zhuang J, Wu Y, Wang P, Zhao G, Liu Y, Jiang X, Gao L, Xia T (2017) Identification of a Flavonoid Glucosyltransferase Involved in 7-OH Site Glycosylation in Tea plants (Camellia sinensis). Sci Rep 7(1):5926

de Souza VR, Pereira PA, da Silva TL, de Oliveira Lima LC, Pio R, Queiroz F (2014) Determination of the bioactive compounds, antioxidant activity and chemical composition of Brazilian blackberry, red raspberry, strawberry, blueberry and sweet cherry fruits. Food Chem 156:362–368

Ding HY (2011) Extracts and constituents of Rubus chingii with 1,1-diphenyl-2-picrylhydrazyl (DPPH) free radical scavenging activity. Int J Mol Sci 12(6):3941–3949

Gachon CM, Langlois-Meurinne M, Henry Y, Saindrenan P (2005) Transcriptional co-regulation of secondary metabolism enzymes in Arabidopsis: functional and evolutionary implications. Plant Mol Biol 58(2):229–245

Giribaldi M, Perugini I, Sauvage FX, Schubert A (2007) Analysis of protein changes during grape berry ripening by 2-DE and MALDI-TOF. Proteomics 7(17):3154–3170

Guo QL, Gao JY, Yang JS (2005) Analysis of Bioactive Triterpenes from Rubus chingii by Cyclodextrin-Modified Capillary Electrophoresis. Chromatographia 62(3–4):145–150

Hamberger B, Hahlbrock K (2004) The 4-coumarate:CoA ligase gene family in Arabidopsis thaliana comprises one rare, sinapate-activating and three commonly occurring isoenzymes. Proc Natl Acad Sci U S A 101(7):2209–2214

Hyun TK, Lee S, Rim Y, Kumar R, Han X, Lee SY, Lee CH, Kim JY (2014) De-novo RNA sequencing and metabolite profiling to identify genes involved in anthocyanin biosynthesis in Korean black raspberry (Rubus coreanus Miquel). PLoS One 9(2):e88292

Jin L, Li X-B, Tian D-Q, Fang X-P, Yu Y-M, Zhu H-Q, Ge Y-Y, Ma G-Y, Wang W-Y, Xiao W-F, Li M (2016) Antioxidant properties and color parameters of herbal teas in China. Ind Crops Prod 87:198–209

Jin P, Wang SY, Gao H, Chen H, Zheng Y, Wang CY (2012) Effect of cultural system and essential oil treatment on antioxidant capacity in raspberries. Food Chem 132(1):399–405

Kim B-G, Sung SH, Ahn J-H (2012) Biological synthesis of quercetin 3-O-N-acetylglucosamine conjugate using engineered Escherichia coli expressing UGT78D2. Appl Microbiol Biotechnol 93(6):2447–2453

Kim JH, Kim BG, Park Y, Ko JH, Lim CE, Lim J, Lim Y, Ahn JH (2006) Characterization of flavonoid 7-O-glucosyltransferase from Arabidopsis thaliana. Biosci Biotechnol Biochem 70(6):1471–1477

Kim SJ, Kim MR, Bedgar DL, Moinuddin SG, Cardenas CL, Davin LB, Kang C, Lewis NG (2004) Functional reclassification of the putative cinnamyl alcohol dehydrogenase multigene family in Arabidopsis. Proc Natl Acad Sci U S A 101(6):1455–1460

Knoch E, Sugawara S, Mori T, Nakabayashi R, Saito K, Yonekura-Sakakibara K (2018) UGT79B31 is responsible for the final modification step of pollen-specific flavonoid biosynthesis in Petunia hybrida. Planta 247(4):779–790

Krauze-Baranowska M, Majdan M, Hałasa R, Głód D, Kula M, Fecka I, Orzeł A (2014) The antimicrobial activity of fruits from some cultivar varieties of Rubus idaeus and Rubus occidentalis. Food Funct 5(10):2536–2541

Kula M, Majdan M, Głód D, Krauze-Baranowska M (2016) Phenolic composition of fruits from different cultivars of red and black raspberries grown in Poland. J Food Compos Anal 52:74–82

Kumar A, Ellis BE (2001) The phenylalanine ammonia-lyase gene family in raspberry. Structure, expression, and evolution. Plant Physiol 127(1):230–239

Lewis DR, Ramirez MV, Miller ND, Vallabhaneni P, Ray WK, Helm RF, Winkel BSJ, Muday GK (2011) Auxin and Ethylene Induce Flavonol Accumulation through Distinct Transcriptional Networks. Plant Physiol 156(1):144–164

Li X, Jin L, Pan X, Yang L, Guo W (2019) Proteins expression and metabolite profile insight into phenolic biosynthesis during highbush blueberry fruit maturation. Food Chem 290:216–228

Li X, Li C, Sun J, Jackson A (2020) Dynamic changes of enzymes involved in sugar and organic acid level modification during blueberry fruit maturation. Food Chem 309:125617

Li X, Luo J, Yan T, Xiang L, Jin F, Qin D, Sun C, Xie M (2013) Deep sequencing-based analysis of the *Cymbidium ensifolium* floral transcriptome. PLoS One 8(12):e85480

Ludwig IA, Mena P, Calani L, Borges G, Pereira-Caro G, Bresciani L, Del RD, Lean ME, Crozier A (2015) New insights into the bioavailability of red raspberry anthocyanins and ellagitannins. Free Radic Biol Med 89:758–769

Mazur SP, Nes A, Wold AB, Remberg SF, Aaby K (2014) Quality and chemical composition of ten red raspberry (Rubus idaeus L.) genotypes during three harvest seasons. Food Chem 160:233–240

Muir SR, Collins GJ, Robinson S, Hughes S, Bovy A, Ric De Vos CH, van Tunen AJ, Verhoeyen ME (2001) Overexpression of petunia chalcone isomerase in tomato results in fruit containing increased levels of flavonols. Nat Biotechnol 19(5):470–474

Noguchi A, Saito A, Homma Y, Nakao M, Sasaki N, Nishino T, Takahashi S, Nakayama T (2007) A UDP-glucose:isoflavone 7-O-glucosyltransferase from the roots of soybean (glycine max) seedlings. Purification, gene cloning, phylogenetics, and an implication for an alternative strategy of enzyme catalysis. J Biol Chem 282(32):23581–23590

Raes J, Rohde A, Christensen JH, Van de Peer Y, Boerjan W (2003) Genome-wide characterization of the lignification toolbox in Arabidopsis. Plant Physiol 133(3):1051–1071

Silber MV, Meimberg H, Ebel J (2008) Identification of a 4-coumarate:CoA ligase gene family in the moss, Physcomitrella patens. Phytochemistry 69(13):2449–2456

Song J, Du L, Li L, Kalt W, Palmer LC, Fillmore S, Zhang Y, Zhang Z, Li X (2015) Quantitative changes in proteins responsible for flavonoid and anthocyanin biosynthesis in strawberry fruit at different ripening stages: A targeted quantitative proteomic investigation employing multiple reaction monitoring. J Proteomics 122:1–10

Stavang JA, Freitag S, Foito A, Verrall S, Heide OM, Stewart D, Sønsteby A (2015) Raspberry fruit quality changes during ripening and storage as assessed by colour, sensory evaluation and chemical analyses. Sci Hortic 195:216–225

Vvedenskaya IO, Vorsa N (2004) Flavonoid composition over fruit development and maturation in American cranberry, Vaccinium macrocarpon Ait. Plant Sci 167(5):1043–1054

Wang SY, Chen C-T, Wang CY (2009) The influence of light and maturity on fruit quality and flavonoid content of red raspberries. Food Chem 112(3):676–684

Wang W, Wang HL, Wan SB, Zhang JH, Zhang P, Zhan JC, Huang WD (2012) Chalcone isomerase in grape vine: gene expression and localization in the developing fruit. Biol Plant 56(3):545–550

Figures

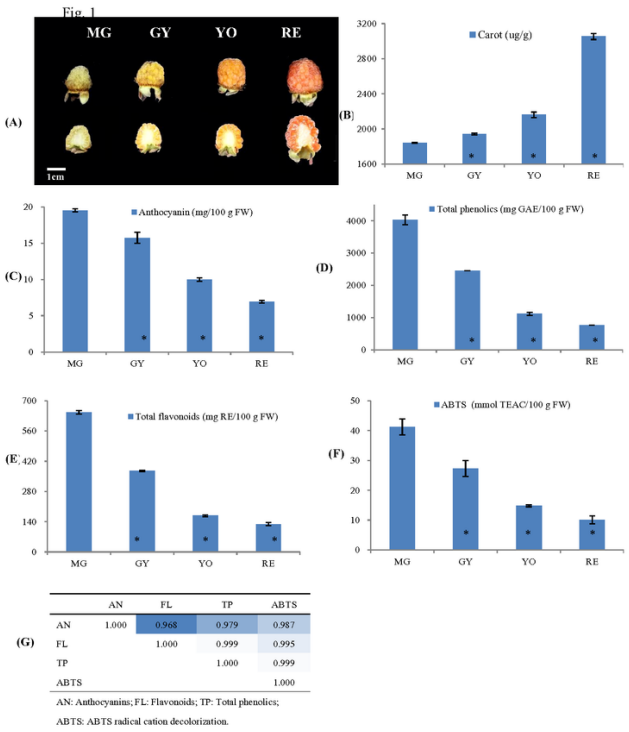

	AN	FL	TP	ABTS
AN	1.000	0.968	0.979	0.987
FL		1.000	0.999	0.995
TP			1.000	0.999
ABTS				1.000

Figure 1

Dynamic change of fruit appearance, phenolic content and antioxidant capacity during maturation in R. chingii. (a) fruit appearance (b) total carotenoid (c) total anthocyanin (expressed as cyanidin 3-glucoside equivalents) (d) total phenolics (e) total flavonoids, (f) the free radical-scavenging activity (ABTS) and (g) pearson correlation between theses patameters (h) mass spetra analysis of anthocyanin compositions. The four typic phases of fruit maturation are MG: mature greeen, GY: green yellow, YO, yellow orange, RE: red. *: significant difference when compared to the one in MG ($P<0.05$).

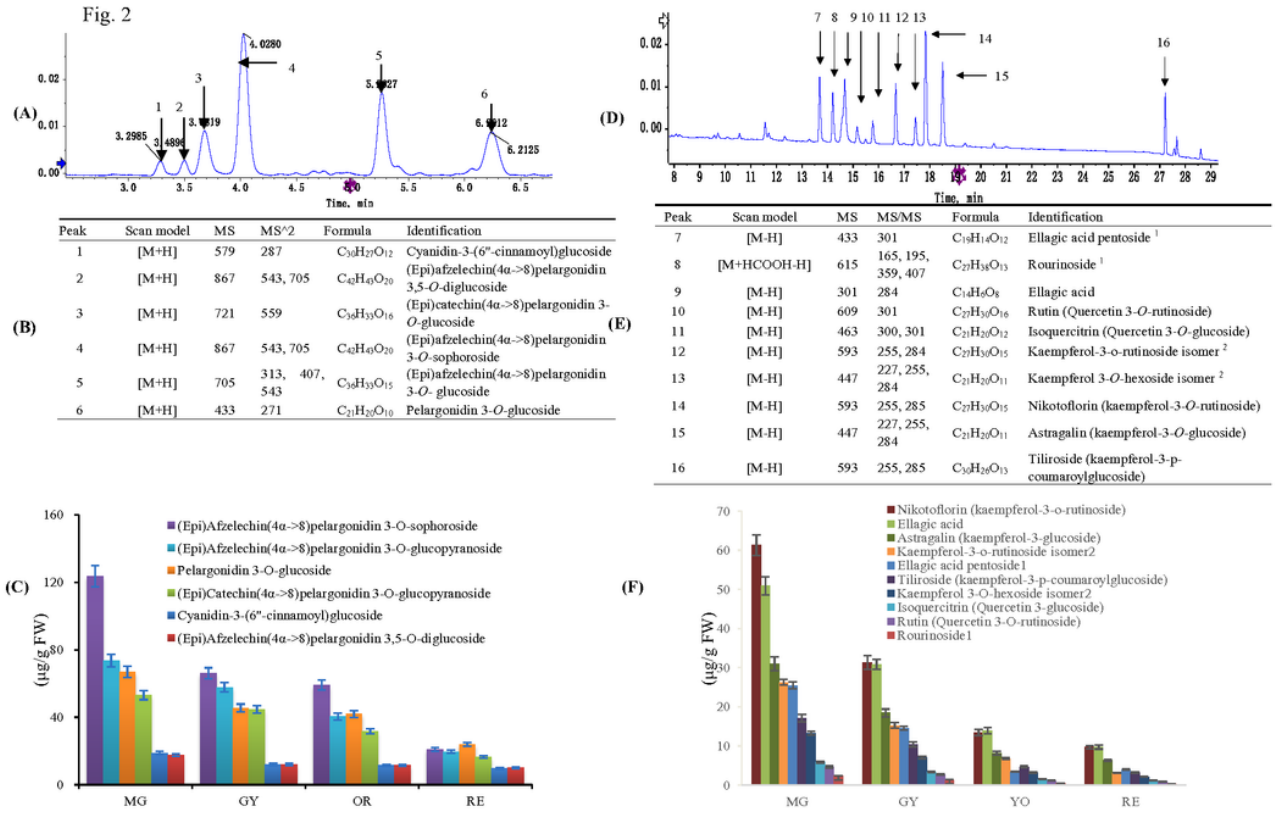

Peak	Scan model	MS	MS^2	Formula	Identification
1	[M+H]	579	287	$C_{30}H_{27}O_{12}$	Cyanidin-3-(6"-cinnamoyl)glucoside
2	[M+H]	867	543, 705	$C_{42}H_{43}O_{20}$	(Epi)afzelechin(4α->8)pelargonidin 3,5-*O*-diglucoside
3	[M+H]	721	559	$C_{36}H_{33}O_{16}$	(Epi)catechin(4α->8)pelargonidin 3-*O*-glucoside
4	[M+H]	867	543, 705	$C_{42}H_{43}O_{20}$	(Epi)afzelechin(4α->8)pelargonidin 3-*O*-sophoroside
5	[M+H]	705	313, 407, 543	$C_{36}H_{33}O_{15}$	(Epi)afzelechin(4α->8)pelargonidin 3-*O*- glucoside
6	[M+H]	433	271	$C_{21}H_{20}O_{10}$	Pelargonidin 3-*O*-glucoside

Peak	Scan model	MS	MS/MS	Formula	Identification
7	[M-H]	433	301	$C_{19}H_{14}O_{12}$	Ellagic acid pentoside [1]
8	[M+HCOOH-H]	615	165, 195, 359, 407	$C_{27}H_{38}O_{13}$	Rourinoside [1]
9	[M-H]	301	284	$C_{14}H_6O_8$	Ellagic acid
10	[M-H]	609	301	$C_{27}H_{30}O_{16}$	Rutin (Quercetin 3-*O*-rutinoside)
11	[M-H]	463	300, 301	$C_{21}H_{20}O_{12}$	Isoquercitrin (Quercetin 3-*O*-glucoside)
12	[M-H]	593	255, 284	$C_{27}H_{30}O_{15}$	Kaempferol-3-o-rutinoside isomer [2]
13	[M-H]	447	227, 255, 284	$C_{21}H_{20}O_{11}$	Kaempferol 3-*O*-hexoside isomer [2]
14	[M-H]	593	255, 285	$C_{27}H_{30}O_{15}$	Nikotoflorin (kaempferol-3-*O*-rutinoside)
15	[M-H]	447	227, 255, 284	$C_{21}H_{20}O_{11}$	Astragalin (kaempferol-3-*O*-glucoside)
16	[M-H]	593	255, 285	$C_{36}H_{26}O_{13}$	Tiliroside (kaempferol-3-p-coumaroylglucoside)

Figure 2

Composition analysis of flavonoid compounds in R. chingii. UPLC spectra of (a) anthocyanins and (d) other flavonoids listed in (b, e); (c, f) the change in their content. Anthocyanin was expressed as pelargonidin 3-O-glucoside equivalents; 1: was expressed as ellagic acid equivalents; 2: was expressed as kaempferol-3-O-rutinoside equivalents

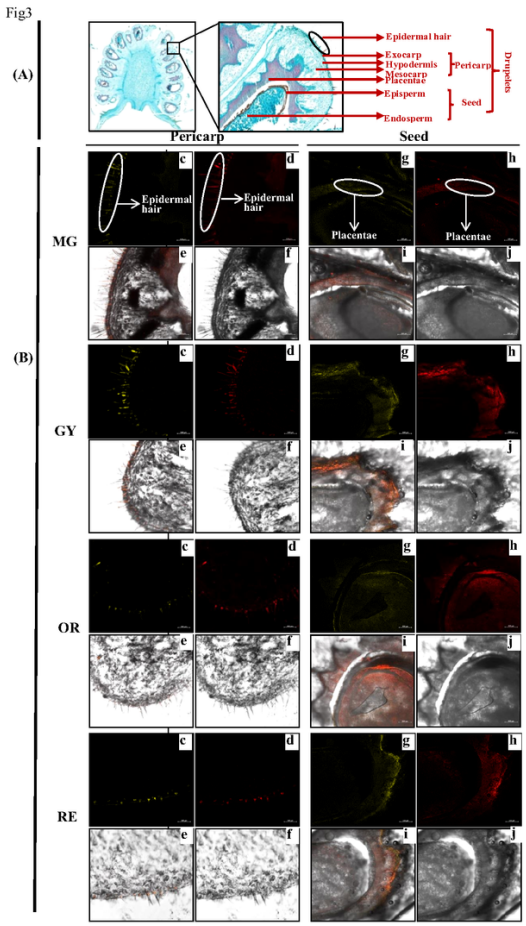

Figure 3

In situ flavonoid staining of fresh-fruit sections at four maturation phases (MG to GY, YO, and RE). (a) Fruit radial sections by paraffin method. (b) Fruit radial sections by frozen method. Fluorescence was collected at (c) 475-504 nm for kaempferol and (d) 577 to 619 nm for quercetin after fresh-fruit section were stained with diphenylboric acid 2-aminoethylester (DPBA) (e) Flavonoid localization in inflorescences combing (c) and (d), (f) original figure without fluorescence. The results showed that flavonoid mainly accumulated in epidermal hair and placentae.

Fig. 4

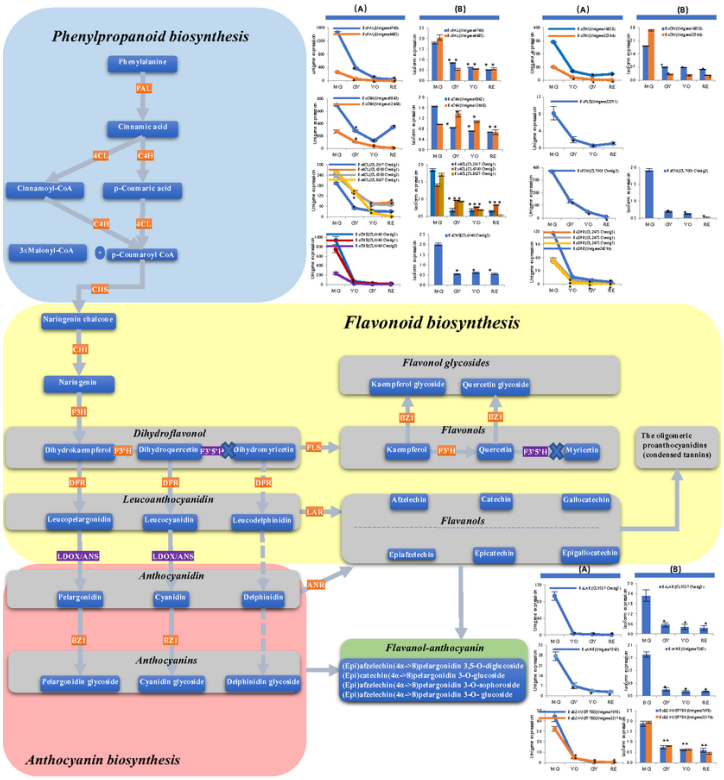

Figure 4

Changes in phenylpropanoid, flavonoid and anthocyanin biosynthesis during four maturation phases in R. chingii. (a) the change of mRNA unigene expression (b) the change of protein isoform expression. RcANS, shown in the purple rectangle, was expressed at a low gene level while RcF3’5’H was not detected at the gene/protein level. Absent expression of RcF3’5’H, shown in the purple rectangle, blocked biosynthesis of the dihydromyricetin, leucodelphinidin, (epi)gallocatechin and their corresponding glycosides. Flavanols and anthocyanins were condensed into flavanol-anthocyanins, shown in the green rectangle.

Supplementary Files

This is a list of supplementary files associated with this preprint. Click to download.

- Supplementalfile.pdf